LC-MS analysis of nitroguanidine and 1-methyl-3-nitroguanidine by catalytic reduction over palladium modified graphitic carbon nitride catalyst

Vitaly Nikolaev[1,2], Sergey Sladkevich[1], Uliana Divina[1], Petr V. Prikhodchenko[2], Guy Gasser[1,3], Luigi Falciola[4], Ovadia Lev[1*]

[1]The Institute Chemistry, The Casali Center of Applied Chemistry, The Hebrew University of Jerusalem, Edmond J. Safra Campus, Jerusalem 9190401, Israel

[2]Kurnakov Institute of General and Inorganic Chemistry, Russian Academy of Sciences, Leninskii prosp. 31, Moscow 119991, Russia

[3]Water Monitoring Laboratory, Israel Water Authority, Rishon Lezion 7528809, Israel

[4] Dipartimento di Chimica, Università degli Studi di Milano, Via Golgi 19, 20133 - Milano – Italy

Corresponding Author: Ovadia Lev, ovadia@huji.ac.il

Vitaly Nikolaev	https://orcid.org/0000-0001-7054-2655
Sergey Sladkevich	https://orcid.org/0000-0002-2486-0078
Uliana Divina	https://orcid.org/0000-0002-6610-9602
Petr V. Prikhodchenko	https://orcid.org/0000-0002-9912-6951
Ovadia Lev	https://orcid.org/0000-0002-3536-2277
Luigi Falciola	https://orcid.org/0000-0002-2031-239X

Abstract

Sensitive analysis of nitro-compounds and particularly those that are not amenable for hydrophobic concentration by solid phase extraction poses an analytical challenge. Nitroguanidine and methyl-nitroguanidine are highly soluble nitramines that detonate on much higher impact and are thus safer compared to RDX. A sensitive method for the determination of nitroguanidine and 1-methyl-3-nitroguanidine by reduction to the respective amines (aminoguanidine and 1-amino-3-methylguanidine which allows subsequent hydrophobization by derivatization by 4-nitrobenzaldehyde followed by LC-ESI-MS analysis is described.

1

Reduction by sodium borohydride over palladium modified graphitic carbon nitride (Pd/g-C$_3$N$_4$) provided improved sensitivity compared to palladium modified activated carbon due to the lower adsorption of the product to the carbon nitride substrate. The limit of detection of the method was 10 ng L^{-1} and the relative standard deviation of six replicates was 5.8 %.

Keywords

nitroguanidine, 1-methyl-3-nitroguanidine, graphitic carbon nitride, aminoguanidine, HPLC-MS

Introduction

Graphitic carbon nitride (g-C$_3$N$_4$) has recently attracted considerable attention. g-C$_3$N$_4$ is a two-dimensional polymer comprised of π-conjugated planar s-triazine rings resembling the layered structure of graphite [1]. High thermal and chemical stability and favorable electronic properties, exploiting the medium-bandgap of g-C$_3$N$_4$, allow its use an as effective heterogeneous catalyst in photocatalytic reactions. g-C$_3$N$_4$ also has several unique properties that allow it to serve as an excellent support for metal catalysts [2]. First, g-C$_3$N$_4$ is hydrophilic and has abundant N-containing functional groups (e.g., −NH$_2$, triazine) that can act as basic coordination sites to facilitate metal nanoparticle (NP) dispersion [3–5]. Second, the surface area and pore size of g-C$_3$N$_4$ can be tailored to promote uniform NP loading [3, 6, 7]. Third, g-C$_3$N$_4$ can be synthesized from abundant precursors (e.g., urea, melamine), and the synthesis process is facile and scalable yielding a stable and environmentally benign material [2, 3, 8].

g-C$_3$N$_4$ modified with noble metals, and especially with Pd NP, show high efficiency for reduction of phenols and their derivatives [8], nitrite and nitrate [2] and nitroarenes [9, 10] and for Suzuki coupling reaction [6]. To date, Pd supported activated carbon (Pd/AC) and charcoal are the most popular supports for palladium nano-grain catalysts for reduction by hydrogen gas, and therefore, the comparison of reduction over Pd/g-C$_3$N$_4$ and Pd/AC catalysts deserve scientific attention. Li et al. [11] showed that the nature of the support plays an important role in the activity and selectivity of Pd catalysts for phenol hydrogenation. The Pd/mpg-C$_3$N$_4$ catalyst gave better activity than commercially available Pd/C, Pd/TiO$_2$, Pd/MgO, Pd/CeO$_2$, and Pd/c-Al$_2$O$_3$, for the hydrogenation of phenol. Cai et al. [12] reported the application of the

Mott–Schottky catalysts based on Pd NPs and g-C_3N_4 (Pd/g-C_3N_4) in the room temperature dehydrogenation of aqueous formic acid. Under similar operating conditions, the catalytic performance of Pd/g-C_3N_4 was found to be orders of magnitudes higher than that of similar Pd/C catalysts. Bhowmik and co-workers described the synthesis of a porous Pd NPs-C_3N_4 composite for hydrogen evolution and hydrogen oxidation reactions in acidic media [13]. Porous Pd NPs/g-C_3N_4 composite showed better hydrogen evolution performance than commercial Pt/C and Pd/C.

In this article, we show that the high efficiency of Pd/g-C_3N_4 can be useful for analytical purposes as well. We compare its performance with a Pd/AC (i.e. Pd/activated carbon) reduction catalyst and show that the former is preferable. We target here the analysis of nitro-explosives, such a nitroguanidine (NQ, Scheme 1) by reduction to the corresponding amine and subsequent hydrophobization to facilitate its concentration/extraction by solid phase extraction (SPE) on hydrophobic cartridges. NQ is a nitramine explosive mostly used as an ingredient in triple base propellants and insensitive munition formulations (e.g. IMX-101), which aims to replace traditional munitions with safer materials in order to improve their stability without compromising other explosive characteristics [14–17]. NQ is intensively used and can be found in areas adjacent to military facilities, where live-fire exercises and controlled explosions are performed [18]. Trace analysis of NQ is a challenge due to its high solubility in water octanol-water partition coefficient (log K_{ow} -0.89), low hydrophobicity, and since it is uncharged in the pH range −0.5 and 12 [19, 20]. The last two attributes make it difficult to concentrate the compound over hydrophobic adsorbents and ion exchange resins.

The NQ derivative, 1-methyl-3-nitroguanidine (MNQ, Scheme 1), which is also studied here is an emerging explosive which is tested alongside NQ in insensitive munition formulations [21–23]. Octanol-water partition coefficient (log K_{ow}) for MNQ is similar to that of NQ, -0.838 [22].

Although the toxicity of NQ and MNQ is rather low for aquatic organisms, their decomposition products can possess higher toxicity compared to the parent compounds, as shown by the increased lethality of microorganisms and aquatic species by the products of UV-degradation of NQ and MNQ [22].

The detection limit of most of the reported analytical techniques for NQ is rather high due to the low extractability of NQ from water, its low retention on the common stationary phase chromatographic columns and the low sensitivity of UV and MS detectors toward NQ. The lowest limit of detection (LOD), 10 ng L^{-1} was demonstrated in our recent work [24]. The reduction of NQ by Zn in acetic acid to aminoguanidine (AQ) followed by the derivatization of the latter with 4-nitrobenzaldehyde (4NBA) to Schiff base was employed prior to LC-MS analysis. The developed method allowed sensitive determination of NQ, though it required a large amount of zinc which has eventually to be discarded as waste. In this article, we demonstrate the catalytic reduction of NQ with Pd/g-C$_3$N$_4$ using NaBH$_4$ as a reducing agent followed by derivatization for sensitive analysis of NQ. This is the first report for the use of Pd/g-C$_3$N$_4$ to improve the analytical preconcentration of a pollutant by subsequent derivatization.

Experimental

Reagents

Nitroguanidine (NQ), aminoguanidine hydrochloride ≥98% (AQ), sodium amide 95%, cyanuric chloride 99%, benzene 99.7%, acridine 97%, potassium chloride, palladium 10 wt% on activated carbon (Pd/AC), palladium(II) chloride 99% were purchased from Sigma (Rehovot, Israel); 1-methyl-3-nitronitroguanidine 98% (MNQ) was purchased from Angene (Holland Moran Ltd, Yehud, Israel). Zinc powder was obtained from Fisher Scientific, and 4-nitrobenzaldehyde 99% (4NBA) and ammonium hydroxide (28-30%) from Alfa Aesar (Holland Moran Ltd, Yehud, Israel). HPLC grade solvents (methanol, ethanol, acetonitrile), glacial acetic acid, formic acid ULC/MS (99%) were purchased from BioLab Ltd (Jerusalem, Israel). All reagents were used without further purification, NQ was dried at 120 °C prior to use.

^{15}N-labeled nitroguanidine, (CH$_4$^{15}N$_4$O$_2$) denoted as ^{15}N$_4$-NQ was synthesized according to [25]. Stock solution (100 mg L^{-1}) of ^{15}N-labeled NQ was prepared by dissolving the compounds in 80 vol% of ethanol in DIW; the solution contained 32.5 mg L^{-1} of ^{15}N$_4$-NQ. Stock standard solution of NQ and AQ (1000 mg L^{-1}) were prepared by dissolving the compound in HPLC-grade methanol. Working solutions of NQ, AQ and ^{15}N-labeled NQ were prepared by dilution of the stock solutions in DIW. The stock solutions were kept refrigerated. Acridine

solution (5.5 mg L^{-1}) was prepared in DIW. 4-Nitrobenzaldehyde (4NBA) was prepared in methanol (10 mg mL^{-1}). Sodium borohydride (0.2 M) was prepared freshly in water before each analysis.

Synthesis of graphitic carbon nitride (g-C$_3$N$_4$)

Synthesis of g-C$_3$N$_4$ was conducted according to [26], and it is described in the "Electronic Supplementary Material".

Synthesis of Pd supported g-C$_3$N$_4$ catalyst (Pd/g-C$_3$N$_4$)

Pd/g-C$_3$N$_4$ was synthesized according to the procedure described in [9]. Briefly, palladium (II) chloride (48 mg) was dissolved in solution of potassium chloride (0.15 M, 13.6 mL) to form orange K$_2$PdCl$_4$ solution. This solution was added slowly to the dispersion of g-C$_3$N$_4$ in DIW (3.33 mg mL^{-1}, 90 mL) with vigorous stirring for 1 h. Sodium borohydride (1 M, 1 mL) was added slowly to the dispersion, and, consequently, the dispersion color changed from pale yellow to grey. After 2 hours the product was collected by centrifugation, washed with DIW and dried at 120 °C for 12 hours.

Instrumentation

Synthesized Pd/g-C$_3$N$_4$ was characterized by Scanning Electron Microscopy, Scanning Transmission Electron Microscopy (STEM) equipped with Energy-dispersive X-ray spectroscopy (EDX) detector, X-ray powder diffraction (XRD), X-ray Photoelectron Spectroscopy (XPS), and Thermal gravimetry (TGA). Detailed information about the equipment is given in the Supporting Information.

Quantitative NQ analysis was performed using Agilent 1200 HPLC coupled to Agilent 6410 triple quadrupole mass spectrometer equipped with electrospray ion source (HPLC-ESI-QQQ-MS/MS), and experimental parameters are listed in Table S1 in the "Electronic Supplementary Material".

High resolution mass spectrometry analysis using Agilent 1100 HPLC coupled to the Agilent 6520A QTOF-MS with electrospray ion source (HPLC-ESI-QTOF-MS) was employed for conclusive identification of reaction products. Experimental parameters of HPLC-ESI-QTOF-MS analysis are given in Table S2 of the "Electronic Supplementary Material".

HPLC with diode array detector (HPLC-DAD) was used for quantitative NQ determination during method optimization procedures and for recovery estimation for different reduction protocols. Experimental parameters of the HPLC-DAD analysis are given in Table S3 of the "Electronic Supplementary Material".

Analytical procedure of NQ analysis

The following procedures represent the optimized conditions for NQ determination. The optimization of the various parameters is described in the corresponding "Results and Discussion" section below.

Reduction of NQ. First, aqueous NQ in the sample was converted to AQ by catalytic reduction over Pd/g-C$_3$N$_4$ with NaBH$_4$ as a reducing agent (Scheme 1). Unless stated otherwise, the catalyst Pd/g-C$_3$N$_4$ (10 μL, 1000 mg L^{-1}), sodium borohydride (0.75 mL, 0.2 M) and ^{15}N-labeled-NQ internal standard (23 μL of 1 mg L^{-1}, to achieve final ^{15}N$_4$-NQ concentration of 75 ng L^{-1}) were added to 10 mL of water sample. The mixture was stirred for 20 min at room temperature and then filtered through a 0.22 μm PTFE syringe filter (Clarinet, Agela Technologies). Acetic acid (0.3 mL) was added under stirring to the solution to remove the excess of sodium borohydride, which can interfere with the upcoming derivatization.

Derivatization of AQ. The optimal derivatization involves the following typical procedure. AQ in the water sample obtained in the reduction step was further converted to AQ-4NBA (Scheme 1) by the reaction with 4-NBA (0.2 mL, 10 mg mL^{-1}). The solution was heated at 75 °C for 40 min under continuous stirring.

Solid Phase Extraction (SPE). After cooling, the samples were neutralized to pH=5.5-6 with ammonium hydroxide. The AQ-4NBA derivate was extracted from the aqueous solution by SPE using a Strata-C18E cartridge (100 mg/3 mL, Phenomenex), which was preconditioned with methanol (6 mL) and DIW (6 mL) consecutively. The sample was loaded into the cartridge and left to percolate by gravity, and then dried for 2 min under vacuum. Target analyte (AQ-4NBA) was subsequently eluted with methanol (6 mL), and the obtained extract was concentrated to a final volume of 0.5 mL by evaporation under nitrogen flow at 65 °C. Acridine was added to the final sample extract as instrument internal standard (5 μL, 5.5 mg L^{-1}).
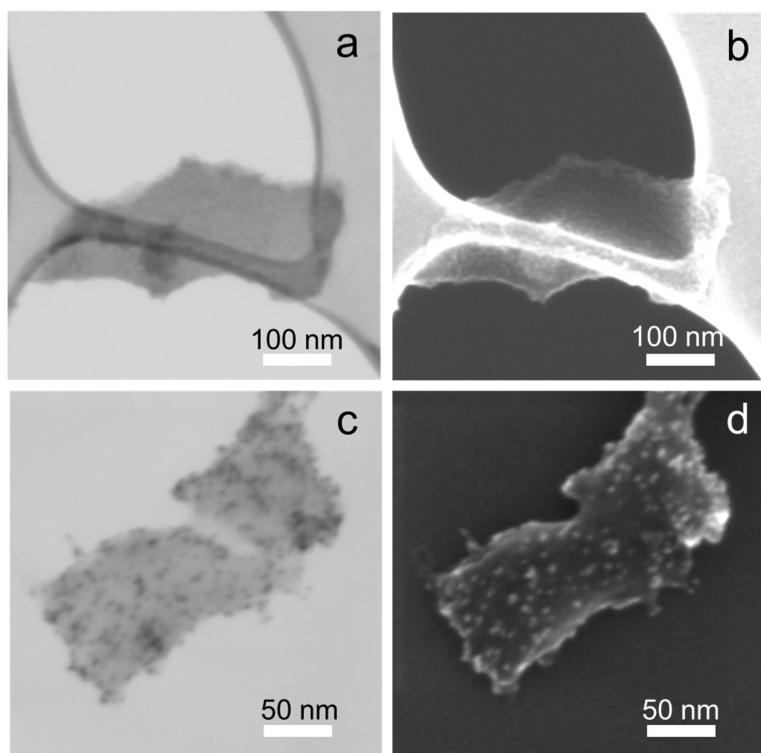
Quantification by HPLC-ESI-QQQ-MS/MS. The analysis was done by injecting 15 μL of the extracted sample with the HPLC autosampler. Chromatographic separation in this and all other HPLC techniques was achieved on Agilent Zorbax Eclipse Plus C18 column (100 mm length, 2.1 mm inner diameter, 3.5 μm particle size). The mobile phase solvents were: (A) 0.1% formic acid in DIW and (B) acetonitrile. The following gradient program for the mobile phase was used: For the time, 0 to 4 min, the composition was set to 5% acetonitrile at 0.2 ml/min flow; from 4 min to 13 min the composition was ramped to 70% acetonitrile and the flow increased to 0.3 ml/min; then the flow and the composition were maintained constant till 17 min; from 17 min to 22 min the composition was ramped to 5% acetonitrile and maintained constant till 26 min; at 26 min the flow was decreased to 0.2 ml/min. Total analysis time was 28 min. MS/MS parameters used for the analysis are given in Table S1 of the "Electronic Supplementary Material". Quantification of NQ was achieved by (i) multipoint linear calibration curve in the range 0.01-25 μg L^{-1} of NQ concentrations or by (ii) 3-point standard additions technique. In both cases $^{15}N_4$-NQ was used as an internal standard.

Field samples. Water samples from several wells near an abandoned industrial area were collected in amber glass bottles. The samples were kept under refrigeration (2-4 °C) prior to the analysis and analyzed by several protocols.

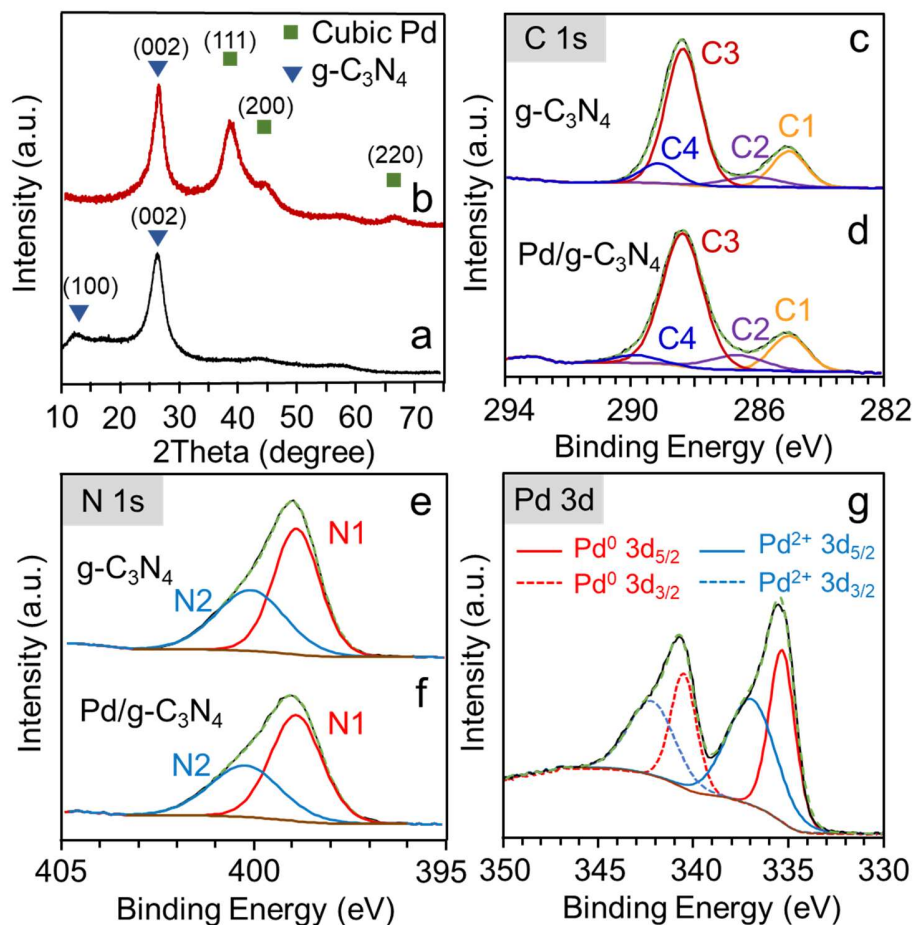## Results and discussion

Characterization of the Pd/g-C₃N₄ catalyst

The micromorphology of g-C₃N₄ and Pd/g-C₃N₄ catalysts was investigated by SEM and STEM Fig. 1(a-d). As illustrated in Fig. 1(a, b), bare g-C₃N₄ shows a sheet structure. The micrographs of Pd/g-C₃N₄ reveal well-dispersed small Pd particles with a mean size of 2.7 nm (Fig. 1c, d), which is in a good correlation with the size of the Pd crystallites calculated from the XRD data (2.6 nm, Table S4).

Fig. 1 STEM (left frames) and SEM (right frames) images of g-C_3N_4 **(a, b)** and Pd/g-C_3N_4 **(c, d).**

Fig. 2(a, b) shows XRD diffractograms of synthesized g-C_3N_4 (curve **a**) and Pd/g-C_3N_4 (curve **b**). The diffraction peaks at 13 and 27.5° correspond to the (100) and (002) lattice planes of g-C_3N_4 [26]. The diffraction peaks at 40, 45.5 and 67° are assigned to the (111), (200) and (220) lattice planes of Pd metal NP, respectively [8]. The (100) reflection is missing in the Pd/g-C_3N_4 diffractogram, and its absence can be explained by the exfoliated nature of carbon nitride after Pd coating, which is previously noted by [27]. The Pd crystallite size is 2.6 nm based on Scherrer's equation for (111) plane (Table S4).

Fig. 2 XRD diffractograms of (a) g-C_3N_4 and (b) Pd/g-C_3N_4; C 1s XPS spectra of (c) g-C_3N_4 and (d) Pd/g-C_3N_4; N 1s XPS spectra of (e) g-C_3N_4 and (f) Pd/g-C_3N_4; Pd 3d spectra of (g) Pd/g-C_3N_4

The obtained XPS spectra are in good agreement with previously reported data [26, 28]. The XPS data confirm the existence of graphite-like sp2 bonded structure in graphitic carbon nitride Fig. 2(c-f). For both bare g-C_3N_4 and Pd/g-C_3N_4 the C 1s peak at 285.0 eV (C1) is ascribed to surface C-C or C=C bonds (Fig.2c, d), whereas the other C 1s peaks at (C2), (C3) and (C4) can be attributed to the C-NH_x, N-C=N and C-O bonds in g-C_3N_4, respectively [28]. The N 1s binding energies in g-C_3N_4 and Pd/g-C_3N_4 may be attributed to the C-N=C (N1) and NH_2 or =NH groups (N2) (Fig. 2e, f) [26]. The nitrogen to carbon ratio in our g-C_3N_4 as estimated based on the XPS data is 58.5 wt % and it is close to the theoretical 60.9 wt%.

The XPS spectrum of Pd 3d (Fig. 2g) presents two peaks for Pd species, and the doublet for each peak is due to the spin-orbital splitting of Pd $3d_{5/2}$ and Pd $3d_{3/2}$ [10]. The peaks at 335.5 and 340.8 eV for Pd $3d_{5/2}$ and Pd $3d_{3/2}$ are ascribed to metallic Pd^0, and those with binding energies 337.1 and 342.3 eV are assigned to Pd^{2+}, which might be present due to surface palladium oxide. Though, according to XPS data, the ratio of Pd^0 to Pd^{2+} is 47/53, this ratio represents the Pd surface, rather than the entire nanoparticle, which are likely to be richer in zero-valent palladium.

Thermogravimetric analysis (Fig. S1) revealed that the residue after 850 °C treatment is 7.7 and 12.7 wt% for the g-C_3N_4 and Pd/g-C_3N_4 respectively, reflecting a difference of only 5%, much lower than the expected 10% difference corresponding to the initial palladium loading during the synthesis. For comparison, the unburned residue for commercial Pd-AC (used in this research to compare its catalytic effectiveness to Pd/g-C_3N_4) with 10 wt% Pd content after 850°C was 12.8 %. Both differences are attributed to the inherent inaccuracy in TGA analysis. Probably the Pd content after heat treatment depends on the Pd presence in the material.

EDX (Energy-dispersive X-ray spectroscopy) studies (Table S4) gave a value of 4.1 wt% for the Pd content in Pd/g-C_3N_4. The difference between the TGA and EDX results are attributed to the inherent imprecision of EDX and the inaccuracy of TGA estimation of the palladium content after heat treatment at 850 °C. For comparison, Pd content in Pd/AC estimated using EDX is 10.2 wt%, whereas the TGA analysis gave a value of 12.8 wt%.
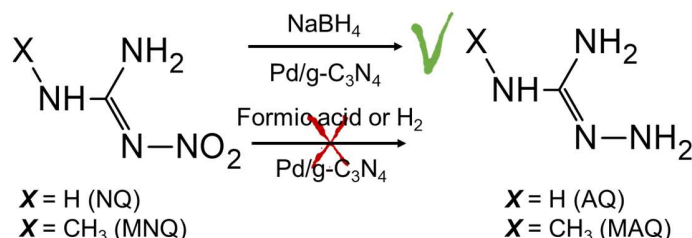
To complete the nanocharacterization of the catalysts, surface area determination by evaluation of the nitrogen adsorption BET isotherms of g-C_3N_4, Pd/g-C_3N_4 and Pd/AC was conducted showing that the surface area of the Pd/g-C_3N_4, 34.8 $m^2 g^{-1}$ is about 50% larger compared to the native g-C_3N_4, but considerably smaller compared to commercial Pd/AC catalyst (Table S4)

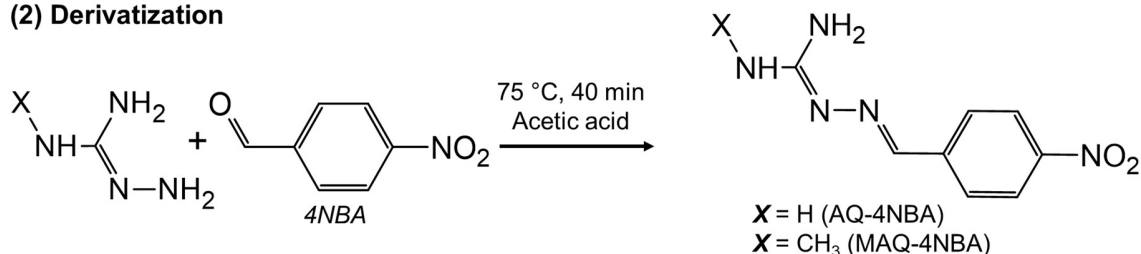**Principle of NQ and MNQ analysis by reduction over Pd/g-C_3N_4 and subsequent derivatization**

The general procedure for the determination of NQ and MNQ is outlined in scheme 1. The first step involves reduction of NQ (or 1-methyl-3-nitroguanidine , MNQ) to the corresponding aminoguanidine (AQ) (or 1-amino-3-methylguanidine (MAQ)) followed by

derivatization with 4-NBA to obtain a more hydrophobic Schiff base, (2-[(4-nitrophenyl)methylene]-hydrazinecarboximidamide) denoted here as AQ-4NBA (or MAQ-4NBA in case of methyl derivative of NQ, Scheme 1)

(1) Reduction

X = H (NQ)
X = CH$_3$ (MNQ)

X = H (AQ)
X = CH$_3$ (MAQ)

(2) Derivatization

4NBA

X = H (AQ-4NBA)
X = CH$_3$ (MAQ-4NBA)

Scheme 1 Schematic illustration of NQ (and MNQ) reduction followed by derivatization with 4NBA

High resolution mass spectrometry analysis was performed to confirm the formation of derivatization products of reduced NQ and MNQ. Fig. S2 shows extracted ion chromatograms for [M+H]$^+$ adducts of AQ-4NBA and MNQ-4NBA obtained from HPLC-ESI-QTOF-MS analysis after the reduction and derivatization of mixed NQ and MNQ aqueous solution (4 mg L^{-1}). Exact masses and mass errors are presented in Table S1 (for AQ-4NBA [M+H]$^+$ adduct m/z 208.0831, mass error -1.0 ppb, for MNQ-4NBA [M+H]$^+$ adduct m/z 222.0989, mass error 1.6 ppb).

The key step in the analysis is the reduction of NQ. Although the reduction on zero-valent zinc in 3% acetic acid was reported [24], the procedure generates a large volume of zinc waste, and an environmentally friendly alternative is preferable. In this article, we examine the reduction over Pd/g-C$_3$N$_4$ and Pd/AC catalysts using several reducing agents: sodium borohydride, formic acid or hydrogen gas (Scheme 1). Although it was shown that hydrogen can be used with Pd-supported catalysts for aqueous phase phenol hydrogenation [8, 11], our attempt to reduce NQ under H$_2$ was unsuccessful. Formic acid is often used as hydrogen donor

11

for catalytic reduction. Xu et al. [10] showed that different nitrobenzene derivatives can be reduced to their corresponding amines by formic acid with Pd supported carbon nitride. However, in the case of NQ, formic acid did not produce the anticipated reduction. Only sodium borohydride demonstrated quick and effective NQ reduction and was chosen as a reducing agent for the rest of the research.

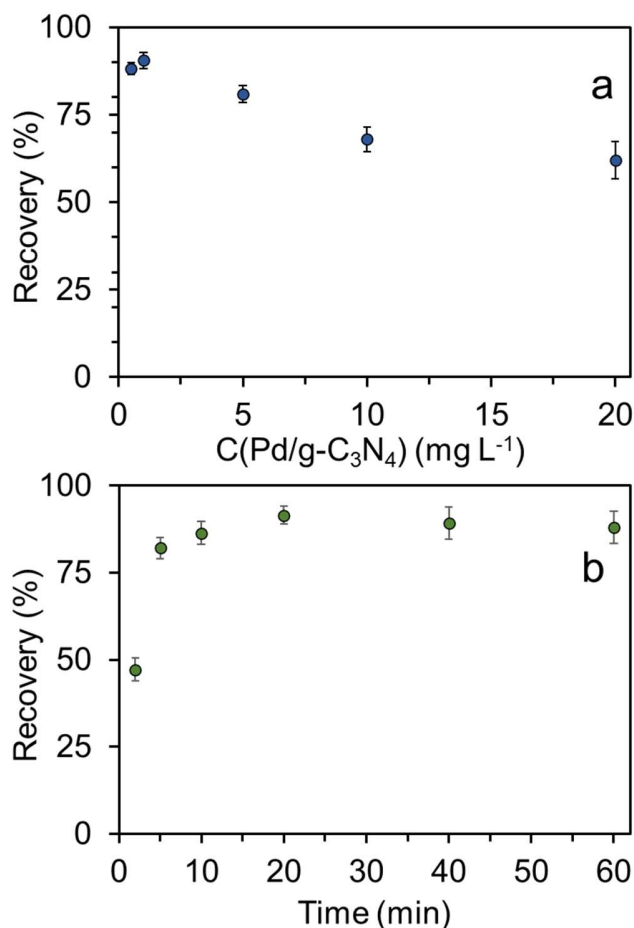**Optimization of the analytical procedure of NQ analysis**

In order to optimize the NQ reduction procedure with sodium borohydride over Pd/g-C_3N_4 catalyst we carried out two set of experiments: (1) in the first set, an estimation of the optimal amount of the Pd/g-C_3N_4 catalyst was performed; and in the second, (2) the optimal time of reduction (over Pd/g-C_3N_4) was established. In the first set of experiments, different amounts of Pd/g-C_3N_4 catalyst (0.5-20 mg L^{-1}) were added to a series of aqueous NQ samples (5 mL, 0.5 mg L^{-1}). Sodium borohydride (15 mM) was added to each sample to start the reduction, and the reaction in each sample was terminated after exactly 20 minutes of stirring by filtering the sample through a 0.22 µm PTFE syringe filter.

In the second set of experiments a constant amount of catalyst (1 mg L^{-1}) was added to a series of aqueous NQ samples (5 mL, 0.5 mg L^{-1}). Sodium borohydride (15 mM) was added to each sample to start the reduction and the reaction in each sample was stopped at a specific time (2-60 min) of stirring by filtering the sample through a 0.22 µm PTFE syringe filter. All tests were performed in triplicates.

HPLC-DAD was used to estimate the recovery of NQ in each test by a 3-point standard addition method (i.e. 4 analyses in total): 0.44 mL of the sample were collected after the reduction step in four separate vials. Glacial acetic acid (0.03 mL) was added to each vial to eliminate the residue of sodium borohydride. Then, different concentrations of AQ (0-0.5 mg L^{-1}) were added to each vial, and derivatization of AQ to AQ-4NBA was achieved by addition of 4NBA (0.02 mL, 10 mg mL^{-1}) and heating in closed vials for 40 min at 75 °C. Acridine was used as an internal standard and was added to each sample (50 µL, 5.5 mg L^{-1}) prior to the HPLC analysis. Final sample volume after the addition of all the components was 0.6 mL.

Fig. 3 shows the dependence of the recovery of NQ quantified as AQ-4NBA versus (a) the concentration of the Pd/g-C_3N_4 at constant reaction time (20 minutes), and (b) as a function

12

of reaction time for constant concentration of g-C_3N_4 (1 mg L^{-1}). It can be noted that optimal conditions are 1 mg L^{-1} and 20 minutes reaction time, though a 10 minutes reaction time gave satisfactory recovery as well.

Fig. 3 Optimization of the NQ reduction over Pd/g-C_3N_4. **(a)** Dependence of NQ recovery on catalyst amount (0.5 mg L^{-1} of NQ, 20 min reaction time); **(b)** Dependence of NQ recovery on time of reduction (0.5 mg L^{-1} of NQ and 1 mg L^{-1} of catalyst). Bars show standard deviation of triplicates

Comparison between different reduction protocols of NQ

Two different approaches to NQ reduction were compared. In the first, reduction over Pd-supported catalysts (either g-C_3N_4 or activated carbon) was tested. In the second approach reduction with Zn in acetic acid was tested (this approach was thoroughly investigated in our recent publication [24]).

In the catalytic reduction tests, the same amount of catalyst, either Pd/g-C$_3$N$_4$ or Pd/AC (1 mg L^{-1}) was added to aqueous NQ sample (0.5 mg L^{-1}). Sodium borohydride (15 mM) was added to each sample to start the reduction. Final volume of each sample was adjusted to 5 mL. The reaction in each sample was stopped after 20 min by filtering the sample through a 0.22 µm PTFE syringe filter. In the Zn reduction test, Zn powder (100 mg) was added to the aqueous NQ solution in 3% (v/v) acetic acid (5 mL, 0.5 mg L^{-1}). The mixture was stirred for 20 min and filtered through 0.22 µm PTFE syringe filter. All samples were prepared in triplicates. HPLC-DAD was used to estimate the recovery of NQ in each test by 3-point standard additions as described in the section "Optimization of the analytical procedure of NQ analysis", vide supra. The NQ recoveries for each reduction protocol are presented in Table 1. Sodium borohydride reduction of NQ over Pd/AC gave very low NQ recovery, which can be explained by the high surface area of carbon, which resulted in considerable sorption of product or reactant on the AC, and lower accessibility of the adsorbed product or reactant to the catalytic palladium grains. The highest NQ recoveries were obtained for catalytic reduction over Pd/g-C$_3$N$_4$ and for the reduction by zinc. However, zinc reduction requires higher loading of reductant (100 times higher) to achieve high recovery in reasonable reaction time.

Table 1 Comparison of recovery of NQ reduction with (i) Zn in acetic acid, (ii) NaBH$_4$ reduction over Pd/AC catalyst; and (iii) by NaBH$_4$ over Pd/g-C$_3$N$_4$ catalyst.

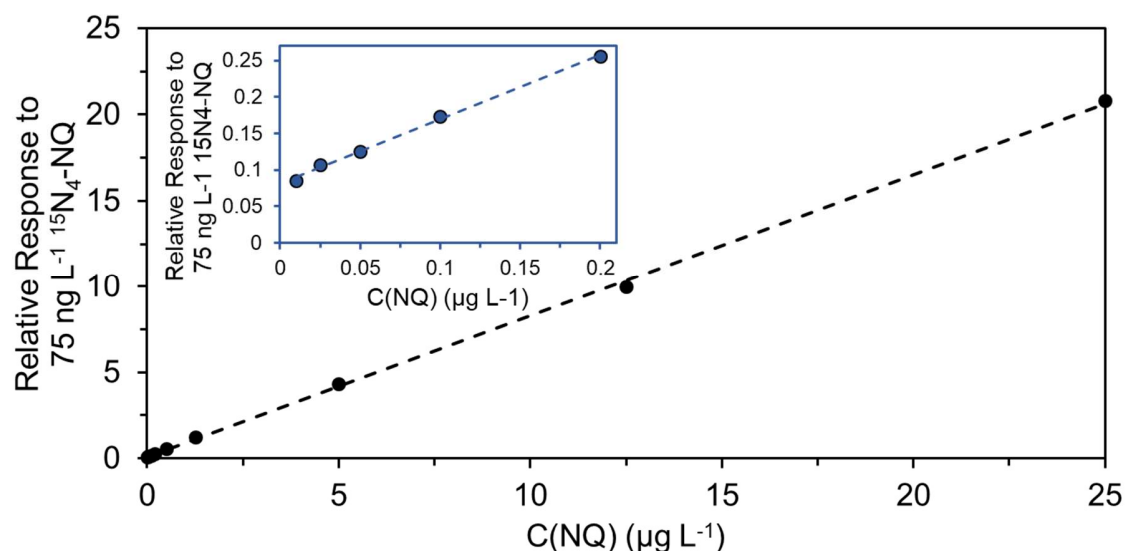| Reduction protocol	Concentration of catalyst (mg L^{-1})	NQ concentration (mg L^{-1})	Recovery*** (%)
(i) Zn*	20000	0.5	93±0.1
(ii) Pd/AC**	1	0.5	28±4.4
(iii) Pd/g-C$_3$N$_4$**	1	0.5	89±2.1

*3 % (by volume) acetic acid

**15 mM aqueous NaBH$_4$

***± standard deviation for triplicates

Analytical performance

In order to investigate the practicality of the developed method, validation parameters, including the linear range of the calibration graph, limit of detection (LOD), limit of

quantification (LOQ), and the correlation coefficient (R^2) were evaluated under optimized extraction conditions. Quantifications were performed with $^{15}N_4$-NQ using either (i) 7-point calibration curve or (ii) 3-point standard addition technique.

Fig. 4 Calibration curve for NQ quantitation using HPLC-ESI-QQQ-MS

Fig. 4 presents the linear calibration curve for the full process of reduction with Pd/g-C_3N_4 and derivatization with 4NBA in the range of NQ concentrations, 0.01-25 µg L^{-1}, giving correlation coefficient R^2=0.9995. The LOD and LOQ of the method were evaluated as 10 ng L^{-1} and 33 ng L^{-1} respectively, and were calculated at 3-times and 10-times the noise level.

Table 2 compares research efforts involving NQ determination, including selected recent publications on NQ analysis using liquid chromatography (LC). As stated, the LOD of most of the reported analytical techniques is rather high. The lowest limit of detection (LOD), 10 ng L^{-1} was demonstrated in our recent work [24], which is comparable with the detection limit of the current method. Repeatability test was performed for six replicates with NQ concentration of 5 µg L^{-1}. Average recovery of 97% was obtained with precision 5.8%.

Table 2 Methods for determination of nitroguanidine (NQ)

Method of analysis	Chromatographic column	Sample preparation	LOD, µg L^{-1}	Reference
HPLC-PDAD[a] (264 nm)	RP[b] C18	Solvent extract from soil	530	[29]

HPLC-ESI(+)-QQQ MS/MS	RP C18	Reduction with Zn followed by derivatization, SPE C18	0.01	[24]
HPLC-PDAD (255 nm)	RP C18	Liquid-liquid extraction	3	[30]
HPLC-UV (263 nm)	RP Hypercarb, HILIC		5	[31]
LC-APCI(-)-QTOF MS/MS	RP C18		5	[32]
UFLC-ESI(-)-Q-MS/MS	RP C18		0.7	[16]
UPLC-ESI-Orbitrap	Hypersil Gold		*	[33]
HPLC-ESI(+)-MS	HydroRP C18, RP biphenyl		9	[34]
HPLC-PAED[c]	RP C18	On-line SPE	20	[35]
HPLC-ESI(+)-QQQ MS/MS	RP C18	catalytic reduction over Pd/g-C_3N_4 followed by derivatization, SPE C18	0.01	this work

[a] Photodiode Array Detector

[b] Reversed phase

[c] Photoassisted electrochemical detection

* LOD was not reported

Field tests

The method was applied to determine NQ concentrations in real water samples from wells located near an industrial site that is known to be contaminated by NQ. Four sampling points were examined (denoted FS1-4 in Fig. S3). The water wells were sampled for NQ analysis. The analysis was conducted using three approaches: (i) 3-point standard addition (spiking the water samples prior to the reduction step with three levels of NQ); (ii) analytical determination based on linear calibration curve for NQ (as described in the "Analytical procedure of NQ analysis" of the "Experimental" section); (iii) using linear calibration curve for NQ after reduction by zinc in acetic acid according to [24]. In all three approaches ^{15}N-labeled NQ was used as the internal standard.

The results of the NQ determination in the real water samples are presented in Table 3. In two of four field samples (denoted as FS1 and FS2 in the schematic map in Fig.S3 in the ESM) NQ was found above the detection limit, and the quantitation performed by the different

quantification approaches gave similar values of NQ. Less than 4% difference between the analysis by full calibration curve (approach (i)) and by standard addition (approach (ii) in Table 3). Less than 15% difference was obtained between the analysis presented in this paper and the analysis by a previously reported method based on zinc reduction in acetic acid. In two other field samples (FS3 and FS4), NQ was not discovered by any of the three methods. Note, that the level of NQ in FS1 and FS2 is below 1 ppb, and therefore determination by reduction/derivatization is vital for the determination of NQ in these wells as can be seen in the LOD values that were reported by other approaches and summarized in Table 2

Table 3 NQ analyses of water samples from the contaminated site by HPLC-ESI-QQQ-MS: comparison of concentrations obtained by isotope dilution calibration curve, standard addition technique, and quantitation after reduction by acetic acid over metallic zinc [24].

NQ concentration µg L^{-1}			
Field sample (FS)	Standard addition (i)	Calibration curve (ii)	Calibration curve (iii)
FS1	0.77	0.75±0.08	0.64
FS2	0.24	0.25±0.05	0.24
FS3	ND	ND	ND
FS4	ND	ND	ND

ND – not detected

Conclusions

NQ determination by reduction to the corresponding amine and subsequent derivatization as presented in this article illuminates two aspects. First it provides an improved analytical method for the determination of NQ (and MNQ), a challenging analyte that has low volatility, low hydrophobicity, low retention in reverse phase chromatography, and low propensity to form ions in the gas phase (i.e. low gas phase protonation affinity and low gas phase acidity), and therefore low sensitivity in LC/MS analysis. A very low detection limit, 10 ng L^{-1} is demonstrated in this article. A second aspect is the use of palladium modified graphitic carbon nitride (Pd/g-C$_3$N$_4$) as a reducing catalyst for chemical analysis. As far as we could find, Pd/g-C$_3$N$_4$ was never used as a pretreatment to improve preconcentration of analytes or as a

mass spectrometry pretreatment, though it has previously reported for electroanalysis. We show in this article, that the much lower Pd/g-C$_3$N$_4$ adsorption capacity for analytes provides an advantage, since it prevents products loss by adsorption on the catalyst. At the same time, g-C$_3$N$_4$ maintains high surface affinity for the small polar compounds, making it better support for Pd-assisted catalysis. This provides an unexpected advantage for the use of Pd/g-C$_3$N$_4$ over the conventional reducing agent, Pd/AC.

Acknowledgements

Conflict of interest. The authors declare that they have no conflict of interest.

References

1.   Wang Y, Wang X, Antonietti M (2012) Polymeric graphitic carbon nitride as a heterogeneous organocatalyst: From photochemistry to multipurpose catalysis to sustainable chemistry. Angew Chemie - Int Ed 51:68–89. https://doi.org/10.1002/anie.201101182

2.   Ye T, Durkin DP, Banek NA, et al (2017) Graphitic Carbon Nitride Supported Ultrafine Pd and Pd-Cu Catalysts: Enhanced Reactivity, Selectivity, and Longevity for Nitrite and Nitrate Hydrogenation. ACS Appl Mater Interfaces 9:27421–27426. https://doi.org/10.1021/acsami.7b09192

3.   Wang L, Wang C, Hu X, et al (2016) Metal/Graphitic Carbon Nitride Composites: Synthesis, Structures, and Applications. Chem - An Asian J 11:3305–3328. https://doi.org/10.1002/asia.201601178

4.   Deng D, Yang Y, Gong Y, et al (2013) Palladium nanoparticles supported on mpg-C$_3$N$_4$ as active catalyst for semihydrogenation of phenylacetylene under mild conditions. Green Chem 15:2525–2531. https://doi.org/10.1039/c3gc40779a

5.   Zhao Z, Sun Y, Dong F (2015) Graphitic carbon nitride based nanocomposites: A review. Nanoscale 7:15–37. https://doi.org/10.1039/c4nr03008g

6.   Zhao Y, Tang R, Huang R (2015) Palladium Supported on Graphitic Carbon Nitride: An Efficient and Recyclable Heterogeneous Catalyst for Reduction of Nitroarenes and Suzuki Coupling Reaction. Catal Letters 145:1961–1971. https://doi.org/10.1007/s10562-015-1600-x

7.   Li XH, Wang X, Antonietti M (2012) Mesoporous g-C_3N_4 nanorods as multifunctional supports of ultrafine metal nanoparticles: Hydrogen generation from water and reduction of nitrophenol with tandem catalysis in one step. Chem Sci 3:2170–2174. https://doi.org/10.1039/c2sc20289a

8.   Wang Y, Yao J, Li H, et al (2011) Highly selective hydrogenation of phenol and derivatives over a pd@carbon nitride catalyst in aqueous media. J Am Chem Soc 133:2362–2365. https://doi.org/10.1021/ja109856y

9.   Nazir R, Fageria P, Basu M, et al (2017) Decoration of Pd and Pt nanoparticles on a carbon nitride (C_3N_4) surface for nitro-compounds reduction and hydrogen evolution reaction. New J Chem 41:9658–9667. https://doi.org/10.1039/c7nj01221g

10.   Xu X, Luo J, Li L, et al (2018) Unprecedented catalytic performance in amine syntheses: Via Pd/g-C_3N_4 catalyst-assisted transfer hydrogenation. Green Chem 20:2038–2046. https://doi.org/10.1039/c8gc00144h

11.   Li Y, Xu X, Zhang P, et al (2013) Highly selective Pd@mpg-C_3N_4 catalyst for phenol hydrogenation in aqueous phase. RSC Adv 3:10973–10982. https://doi.org/10.1039/c3ra41397g

12.   Cai YY, Li XH, Zhang YN, et al (2013) Highly efficient dehydrogenation of formic acid over a palladium- nanoparticle-based mott-schottky photocatalyst. Angew Chemie - Int Ed 52:11822–11825. https://doi.org/10.1002/anie.201304652

13.   Bhowmik T, Kundu MK, Barman S (2016) Palladium Nanoparticle-Graphitic Carbon Nitride Porous Synergistic Catalyst for Hydrogen Evolution/Oxidation Reactions over a Broad Range of pH and Correlation of Its Catalytic Activity with Measured Hydrogen Binding Energy. ACS Catal 6:1929–1941. https://doi.org/10.1021/acscatal.5b02485

14.   Oxley JC, Smith JL, Donnelly MA, et al (2016) Thermal Stability Studies Comparing IMX-101 (Dinitroanisole/Nitroguanidine/NTO) to Analogous Formulations Containing Dinitrotoluene. Propellants, Explos Pyrotech 41:98–113. https://doi.org/10.1002/prep.201500150

15.   Koch EC (2019) Insensitive High Explosives: III. Nitroguanidine – Synthesis – Structure – Spectroscopy – Sensitiveness. Propellants, Explos Pyrotech 44:267–292. https://doi.org/10.1002/prep.201800253

16.   Mu R, Shi H, Yuan Y, et al (2012) Fast separation and quantification method for nitroguanidine and 2,4-dinitroanisole by ultrafast liquid chromatography-tandem mass spectrometry. Anal. Chem. 84:3427–3432

17.   Stalcup H, Williams RW (1955) Volumetric Determination of Nitrocellulose and Nitroguanidine By Transnitration of Salicylic Acid. Anal Chem 27:543–546. https://doi.org/10.1021/ac60100a015

18.   Walsh MR, Walsh ME, Ampleman G, et al (2012) Munitions propellants residue deposition rates on military training ranges. Propellants, Explos Pyrotech 37:393–406. https://doi.org/10.1002/prep.201100105

19.   DeVries JE, Gantz ESC (1954) Spectrophotometric Studies of Dissociation Constants of Nitroguanidines, Triazoles and Tetrazoles. J Am Chem Soc 76:1008–1010. https://doi.org/10.1021/ja01633a019

20.   Lockhart JC (1957) Bonner and Lockhart: The Denitration

21.   Kinkead ER, Wolfe RE, Salins SA, et al (1993) N-Methyl-N'-Nitroguanidine: Irritation, Sensitization, and Acute Oral Toxicity, Genotoxicity, and Methods for Analysis in Biological Samples. Toxicol Ind Health 9:457–477. https://doi.org/10.1177/074823379300900305

22.   Lotufo GR, Gust KA, Ballentine ML, et al (2020) Comparative Toxicological Evaluation of UV-Degraded versus Parent-Insensitive Munition Compound 1-Methyl-3-Nitroguanidine in Fathead Minnow. Environ Toxicol Chem 39:612–622. https://doi.org/10.1002/etc.4647

23.   Roos BD (2014) (12) United States Patent. 1:

24.   Voloshenko Rossin A, Sladkevich S, Gasser G, et al (2017) Sensitive Analysis of Nitroguanidine in Aqueous and Soil Matrices by LC-MS. Anal Chem 89:9990–9996. https://doi.org/10.1021/acs.analchem.7b02364

25.   Bulusu S, Dudley RL, Autera JR (1987) Structure of nitroguanidine: Nitroamine or nitroimine? New NMR evidence from 15N-labeled sample and 15N spin coupling constants. Magn Reson Chem 25:234–238. https://doi.org/10.1002/mrc.1260250311

26.   Guo Q, Xie Y, Wang X, et al (2003) Characterization of well-crystallized graphitic carbon nitride nanocrystallites via a benzene-thermal route at low temperatures. Chem Phys Lett 380:84–87. https://doi.org/10.1016/j.cplett.2003.09.009

27.   Qiu P, Chen H, Xu C, et al (2015) Fabrication of an exfoliated graphitic carbon nitride as a highly active visible light photocatalyst. J Mater Chem A 3:24237–24244. https://doi.org/10.1039/c5ta08406g

28.   Liu J, Wei Z, Fang W, et al (2019) Enhanced Photocatalytic Hydrogen Evolution of the Hydrogenated Deficient g-C_3N_4 via Surface Hydrotreating. ChemCatChem 11:6275–6281. https://doi.org/10.1002/cctc.201900284

29.   Temple T, Cipullo S, Galante E, et al (2019) The effect of soil type on the extraction of insensitive high explosive constituents using four conventional methods. Sci Total Environ 668:184–192. https://doi.org/10.1016/j.scitotenv.2019.02.359

30.   Jyot G, Singh B (2017) Development and validation of an HPLC method for determination of thiamethoxam and its metabolites in cotton leaves and soil. J AOAC Int 100:796–803. https://doi.org/10.5740/jaoacint.16-0206

31.   Walsh ME (2016) Analytical Methods for Detonation Residues of Insensitive Munitions. J Energ Mater 34:76–91. https://doi.org/10.1080/07370652.2014.999173

32.   DeTata D, Collins P, McKinley A (2013) A fast liquid chromatography quadrupole time-of-flight mass spectrometry (LC-QToF-MS) method for the identification of organic explosives and propellants. Forensic Sci Int 233:63–74. https://doi.org/10.1016/j.forsciint.2013.08.007

33.   Richard T, Weidhaas J (2014) Dissolution, sorption, and phytoremediation of IMX-101 explosive formulation constituents: 2,4-dinitroanisole (DNAN), 3-nitro-1,2,4-triazol-5-one (NTO), and nitroguanidine. J Hazard Mater 280:561–569. https://doi.org/10.1016/j.jhazmat.2014.08.042

34.   Russell AL, Seiter JM, Coleman JG, et al (2014) Analysis of munitions constituents in IMX formulations by HPLC and HPLC-MS. Talanta 128:524–530. https://doi.org/10.1016/j.talanta.2014.02.013

35.   Marple RL, LaCourse WR (2005) Application of photoassisted electrochemical detection to explosive-containing environmental samples. Anal Chem 77:6709–6714. https://doi.org/10.1021/ac050886v